# Age of Information: An Indirect Way To Improve Control System Performance

Onur Ayan*, Anthony Ephremides†, Wolfgang Kellerer*
*Chair of Communication Networks, Technical University of Munich, Munich, Germany
†Electrical and Computer Engineering Department, University of Maryland, College Park, MD
Email:{onur.ayan, wolfgang.kellerer}@tum.de, etony@umd.edu

***Abstract*—In this paper, we consider $N$ heterogeneous control sub-systems sharing a wireless communication channel. Network resources are limited and they are allocated by a centralized scheduler. Each transmission is lost with a probability that is higher or lower depending on the portion each sub-system receives from the pool of network resources. Furthermore, state measurements go through a first come first serve (FCFS) Geo/Geo/1 transmission queue after they are generated by each sensor. In such a setting, the information at each remote controller that is observing the state measurements through the wireless channel gets outdated. Age of Information (AoI) captures this effect and measures the information freshness at each controller. By definition, AoI is control unaware thus not a standalone metric to capture the heterogeneous requirements of control sub-systems. However, we show how the stationary distribution of Age of information (AoI) can be employed as an intermediate metric to obtain the expected control performance in the network. As a result, we solve the resource allocation problem optimally and show by simulations that we are able to improve the control performance indirectly through AoI.**

***Index Terms*—Age of Information, Stationary Distribution, Networked Control Systems, Remote Estimation**

## I. Introduction

With the ongoing advances in computing, communications and process control, cyber-physical systems (CPS) are envisioned to constitute a serious portion of the data traffic in communication networks. Environmental monitoring and control, collision avoidance for autonomous driving, distributed robotics, manufacturing and smart structures are some of the most prominent examples of CPS [1]. From a system theoretical perspective, such applications can be classified as feedback control loops that are closed over a communication network, i.e., *networked control systems (NCS)*.

A typical NCS scenario consists of multiple sensors that measure the system state of their control processes and transmit the generated data over a shared wireless network where resources are limited. As in a great portion of current communication systems, the sensory data might be queued before being transmitted. This leads to the destination receiving delayed information that were backlogged in the transmission queue of the source. Additionally, the packets carrying the status updates can be lost due to the lossy nature of wireless transmissions. As a result, this leaves the monitoring application, the control process in our case, to deal with outdated data and make decisions based on less reliable information.

Particularly, since we are dealing with real-time applications that rely on fast and regular exchange of data, the achieved performance of NCS applications deteriorates as the network induces additional delays and packet losses. In such a setting, to measure how well the communication network is performing with respect to providing regular and prompt status updates, *age of information (AoI)* has been proposed as a metric to quantify information freshness in remote monitoring scenarios such as NCS [2].

By definition, AoI measures the time that has elapsed since the generation of the freshest information available at the receiver monitoring a remote process. It has been adopted as a cross-layer metric to redesign different layers of communication network to increase information freshness in the network. In particular, the vast majority of AoI research focuses on minimizing average AoI in various settings such as in single-hop queuing systems [3], [4] or multi-hop networks [5], [6]. In addition to focusing on average performance of age, there have been recent attempts to go one step further and derive distributions of age both in single-hop queuing systems [7], [8] and multi-hop simple line networks [9], [10].

From the existing literature, we know that minimizing AoI as a standalone metric is sub-optimal when it comes to NCS scenarios with heterogeneous control loops [11]. Therefore, control-aware age-penalty functions have been derived and employed to take optimal decisions [12]–[14] in wireless networked control systems. In [12] authors study a centralized resource allocation problem for multiple, heterogeneous feedback control loops. They consider an NCS scenario where each transmission is lost with a probability that is time-invariant. Under the assumption that sensors are able to replace outdated packets in their transmission queue, they obtain an optimal, stationary scheduling policy by solving a discounted cost minimization problem. In [13] and [14] authors derive optimal sampling policies in the context of NCS, where they employ control dependent age-penalty functions as a metric. Similar to [12], those works assume that sensors are always able to replace any outdated packet in the transmission queue with a fresher incoming packet and thus assume zero queuing delay.

To the best of our knowledge, none of the existing works study a resource allocation problem for NCS where the sensor data has to go first through a first come first serve (FCFS) transmission queue, which is a very commonly found scenario

in current communication devices. Rate allocation for NCS with queuing has been tackled before in [15], however only under the assumption that there are no packet losses in the network.

### A. Our Contribution

In the present work, we study a resource allocation problem where a wireless channel is shared by multiple, heterogeneous feedback control sub-systems. The observation data measured by sensors of each sub-system need to go through a Geo/Geo/1 discrete time queue with FCFS discipline. The limited resources of the wireless network is distributed by a centralized entity which in turn determines the success probability of individual sub-systems. Leveraging the results of [7], which provides a stationary distribution of age in discrete time queuing systems, we show how distributions of AoI can be applied to solve the scheduling problem optimally in order to maximize control performance in NCS.

### B. Notation

Vectors and matrices are written in small and capital bold letters, respectively, i.e., $\boldsymbol{v} \in \mathbb{R}^n$ and $\boldsymbol{M} \in \mathbb{R}^{n \times m}$. $\boldsymbol{M}^T$ denotes the transpose of a matrix $\boldsymbol{M}$. Moreover, $\boldsymbol{M}^p$ represents the $p$-th power of $\boldsymbol{M}$. $\mathtt{tr}(\cdot)$ is the trace operator.

## II. System Model

### A. Network Model

Suppose a communication network that is comprised of $N$ independent, linear time-invariant (LTI) control sub-systems. Each sub-system consists of a plant $\mathcal{P}_i$, a sensor $\mathcal{S}_i$ and a controller $\mathcal{C}_i$, where each $\mathcal{S}_i$ is co-located with $\mathcal{P}_i$ and observes the system state via an ideal link. The sensor information is transmitted to $\mathcal{C}_i$ in a single packet over the wireless sensor-to-controller link. The controller is responsible for calculating the control input to drive the plant state to any desired reference value with the help of incoming sensor observations. We assume time to be slotted with slot durations normalized to unity. Throughout the paper, we use $t \in \mathbb{N}_0$ for time slot indexing and $i = \{1, 2, \ldots, N\}$ for sub-system indexing.

Any packet transmission starting in slot $t$ ends within the same slot. Moreover, each wireless sensor-to-controller link is prone to packet losses and we model it as an erasure channel with a packet success probability of $\mu_i$. In our system, allocation of network resources is decided by a central entity before operation that defines the constant packet success probability for each sub-system. One can imagine it as the distribution of multiple channels that are limited in amount among sub-systems, where each sub-system transmits multiple copies of the same packet simultaneously on different channels that are assigned to it. The probability that at least one of those transmissions is successful defines the aggregated success probability of the wireless sensor-to-controller link, i.e., $\mu_i$. For the rest of our analysis, we approximate the behavior of such a wireless link with limited amount of resources with the following constraints:

$$\sum_{i=1}^{N} \mu_i \leq R, \qquad 0 \leq \mu_i \leq 1, \forall i, \tag{1}$$

where $R \in \mathbb{R}$ is the total capacity. Note that $R$ is a constant scalar only under the assumption that packet success probabilities behave linearly between zero and one, which is what we assume here.

We suppose that sensors have a packet queue of infinite capacity to accommodate the state measurements. At the beginning of each time slot $t$, each $\mathcal{S}_i$ observes the plant state. However, we assume that sensors posses limited computational capability thus each measurement is injected into the packet queue with a probability of $0 \leq \lambda_i \leq 1$ without any further processing. In addition, each queue operates under FCFS discipline and any information is retransmitted until at least one of its copies is successfully received by the controller[1]. As a result, the queue can be modeled as a Geo/Geo/1 discrete time queue with service rate $\mu_i$.

### B. Control Model

We represent the behavior of the $i$-th control sub-system with LTI model in discrete time:

$$\boldsymbol{x}_i[t+1] = \boldsymbol{A}_i \boldsymbol{x}_i[t] + \boldsymbol{B}_i \boldsymbol{u}_i[t] + \boldsymbol{w}_i[t], \tag{2}$$

with time-invariant system matrix $\boldsymbol{A}_i \in \mathbb{R}^{n_i \times n_i}$ and input matrix $\boldsymbol{B}_i^{n_i \times m_i}$. The system state $\boldsymbol{x}_i \in \mathbb{R}^{n_i}$ is fully observable by $\mathcal{S}_i$ and $\boldsymbol{u}_i \in \mathbb{R}^{m_i}$ is the control input. Moreover, $\boldsymbol{w}_i \in \mathbb{R}^{n_i}$ denotes the system noise acting on the state dynamics of the source that is characterized by a multi-variate Gaussian distribution with zero mean and a diagonal covariance matrix $\boldsymbol{\Sigma}_i \in \mathbb{R}^{n_i \times n_i}$, i.e., $\boldsymbol{w}_i \sim \mathcal{N}(\boldsymbol{0}, \boldsymbol{\Sigma}_i)$.

In order to compensate for the delays and losses in the network, $\mathcal{C}_i$ employs an estimator that estimates the current state given the observation history until $t$. Under the assumption that $\mathcal{C}_i$ is aware of the time-invariant system parameters $\boldsymbol{A}_i$, $\boldsymbol{B}_i$ and $\boldsymbol{\Sigma}_i$, the estimated plant state is obtained from:

$$\begin{aligned} \hat{\boldsymbol{x}}_i[t] &\triangleq \mathbb{E}\left[\boldsymbol{x}_i[t] \mid \boldsymbol{x}_i[\nu_i(t)]\right] \\ &= \boldsymbol{A}_i^{t-\nu_i(t)} \boldsymbol{x}_i[\nu_i(t)] + \sum_{q=1}^{t-\nu_i(t)} \boldsymbol{A}_i^{q-1} \boldsymbol{B}_i \boldsymbol{u}_i[t-q], \end{aligned} \tag{3}$$

where $\nu_i[t]$ is the generation time step of the most recent information available at $\mathcal{C}_i$. The proof is given in appendix A. Following an estimation at each time step, the controller determines the control input with the following *control law*:

$$\boldsymbol{u}_i[t] = -\boldsymbol{L}_i^* \hat{\boldsymbol{x}}_i[t], \tag{4}$$

where $\boldsymbol{L^*}_i \in \mathbb{R}^{m_i \times n_i}$ denotes the optimal state feedback gain matrix. $\boldsymbol{L^*}_i$ is obtained from:

$$\boldsymbol{L^*}_i = \left(\boldsymbol{R}_i + \boldsymbol{B}_i^T \boldsymbol{P}_i \boldsymbol{B}_i\right)^{-1} \boldsymbol{B_i}^T \boldsymbol{P}_i \boldsymbol{A}_i, \tag{5}$$

[1]This implies that we assume an underlying ACK/NACK feedback system for each packet in the transmission queue

which is the solution of the discrete time algebraic Riccati equation:

$$\boldsymbol{P}_i = \boldsymbol{Q}_i + \boldsymbol{A}_i^T \left(\boldsymbol{P}_i - \boldsymbol{P}_i \boldsymbol{B}_i \left(\boldsymbol{R}_i + \boldsymbol{B}_i^T \boldsymbol{P}_i \boldsymbol{B}_i\right)^{-1} \boldsymbol{B}_i^T \boldsymbol{P}_i\right) \boldsymbol{A}_i. \tag{6}$$

Here, $\boldsymbol{Q}_i$ and $\boldsymbol{R}_i$ are weighting matrices of appropriate size that penalize the state and control inputs in the infinite horizon, linear-quadratic-Gaussian (LQG) cost function $F_i$:

$$F_i = \frac{1}{T} \limsup_{T\to\infty} \sum_{t=0}^{T-1} (\boldsymbol{x}_i[t])^T \boldsymbol{Q}_i \boldsymbol{x}_i[t] + (\boldsymbol{u}_i[t])^T \boldsymbol{R}_i \boldsymbol{u}_i[t]. \tag{7}$$

$F_i$ is an indicator of control performance that is commonly used in control theory textbooks and in the literature [15]. The lower $F_i$ is, the higher is the *quality of control (QoC)*.

Note that, the controller gain $\boldsymbol{L}^*$ is independent of the network. There are controllers in the literature that take network delay or packet loss into account to increase the control performance. However, this is beyond the scope of this work. Therefore, we assume that the controller design takes place prior to deployment.

## III. Mean Squared Error Optimal Resource Allocation

### A. Estimation Error and Age of Information

Given the system model introduced in the previous section and the control law as in Eq. (3) and (4), let us define the *network-induced error (NIE)* as the difference between the system state and the remotely estimated state, that is:

$$\boldsymbol{e}_i[t] \triangleq \boldsymbol{x}[t] - \hat{\boldsymbol{x}}[t]. \tag{8}$$

NIE is defined as the deviation of the real state of $\mathcal{P}_i$ from the estimated state at $\mathcal{C}_i$. As the NIE decreases, we consider the estimation to be more accurate. The estimation performance is measured with the mean squared error (MSE), i.e., $\mathbb{E}\left[\|\boldsymbol{e}_i[t]\|^2\right] = \mathbb{E}\left[(\boldsymbol{e}_i[t])^T \boldsymbol{e}_i[t]\right]$. Given the freshest plant state $\boldsymbol{x}[\nu_i[t]]$ that corresponds to the system state at $\nu_i[t]$ and available at $\mathcal{C}_i$ by $t$, one can determine MSE from Eq. (2), (3) and (8) as:

$$\mathbb{E}\left[\|\boldsymbol{e}_i[t]\|^2 \mid \boldsymbol{x}_i[t], \hat{\boldsymbol{x}}_i[t]\right] = \sum_{p=0}^{t-\nu_i[t]-1} \mathsf{tr}\left(\left(\boldsymbol{A}_i^T\right)^p \boldsymbol{A}_i \boldsymbol{\Sigma}_i\right). \tag{9}$$

Proof can be found in appendix B. It is important to mention that the number of summands in (9) depends on $t-\nu_i[t]$ while the summands are composed of time-invariant elements, i.e., $\boldsymbol{A}_i, \boldsymbol{\Sigma_i}$ are constant matrices. We define the number of time steps that have elapsed since the generation of the most recent information that is available to $\mathcal{C}_i$ as AoI, i.e.:

$$\Delta_i[t] \triangleq t - \nu_i[t]. \tag{10}$$

As a result, we are able to define an *age-penalty function* $g_i(\Delta_i) : \mathbb{N} \to \mathbb{R}$ of the form:

$$g(\Delta_i) = \sum_{p=0}^{\Delta_i-1} \mathsf{tr}\left(\left(\boldsymbol{A}_i^T\right)^p \boldsymbol{A}_i \boldsymbol{\Sigma}_i\right). \tag{11}$$

that maps age to mean squared error.

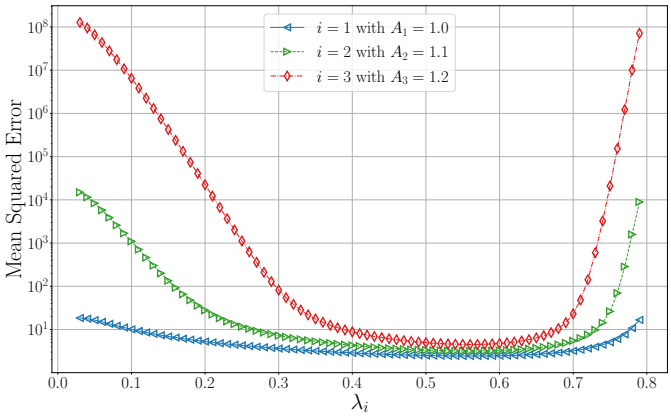


Fig. 1. MSE for varying $\lambda_i$ while the service rate is fixed, i.e., $\mu_i = 0.8, \forall i$, is fixed. Different colors represent different type of control systems with system matrices $A_{1,2,3} \in \{1.0, 1.1, 1.2\}$. A higher $A_i$ represents a less stable system that is more challenging to control.

### B. Stationary Distribution of AoI in a Geo/Geo/1 Queue

From the literature, we know that while communicating through a FCFS Geo/Geo/1 queue, AoI follows a stationary distribution [7]. Given the arrival and service rate of a Geo/Geo/1 queue, i.e., $\lambda_i$ and $\mu_i$ with $\frac{\lambda_i}{\mu_i} = \rho_i < 1$, for random variable $\Delta$ as AoI, the probability of having $\Delta = \delta$ is given as[2]:

$$\Pr[\Delta = \delta] = \frac{(\mu_i - \lambda_i)\left(\frac{1-\lambda_i}{1-\mu_i}\right)^{-\delta}}{1-\mu_i} - \lambda_i\mu_i\delta(1-\mu_i)^{\delta-1} + \frac{\lambda_i\mu_i(1-\lambda_i)^{\delta}}{\mu_i - \lambda_i} + \frac{\left(\lambda_i^2 - \lambda_i\mu_i(\mu_i+1) + \mu_i^2\right)(1-\mu_i)^{\delta-1}}{\lambda_i - \mu_i}. \tag{12}$$

As a result, we can obtain the MSE as defined in Eq. (11) by applying fundamental theory of expectations [16, p. 379]:

$$\begin{aligned} C_i(\lambda_i, \mu_i) &= \lim_{\tau\to\infty} \frac{1}{\tau} \sum_{t=0}^{\tau-1} \boldsymbol{e}_i^T(t)\boldsymbol{e}_i(t) \\ &= \sum_{\delta=1}^{\infty} \Pr[\Delta_i = \delta] \cdot g_i(\delta) \\ &= \sum_{\delta=1}^{\infty} \Pr[\Delta_i = \delta] \cdot \sum_{p=0}^{\delta-1} \mathsf{tr}\left((\boldsymbol{A}_i^T)^p (\boldsymbol{A}_i)^p \boldsymbol{\Sigma}_i\right) \end{aligned} \tag{13}$$

Next, we can plot the MSE against arrival/service rate while the remaining parameter is fixed. For instance, Fig. 1 shows how the mean squared error changes for 3 different classes of scalar control sub-systems with different system matrices $A_{1,2,3} = \{1.0, 1.1, 1.2\}$. Note that the packet injection probability $\lambda_i$ is varied while the packet success probability $\mu_i$ is kept constant at $\mu_i = 0.8, \forall i$. We observe that MSE is high for low $\lambda_i$ due to increased inter arrival times which shows

[2]Note that Eq. (12) is a shifted version of the original equation in [7], as we allow $\Delta = 1$ as the minimum AoI in our system while they assume $\Delta = 2$ as the minimum possible age after a successful transmission.

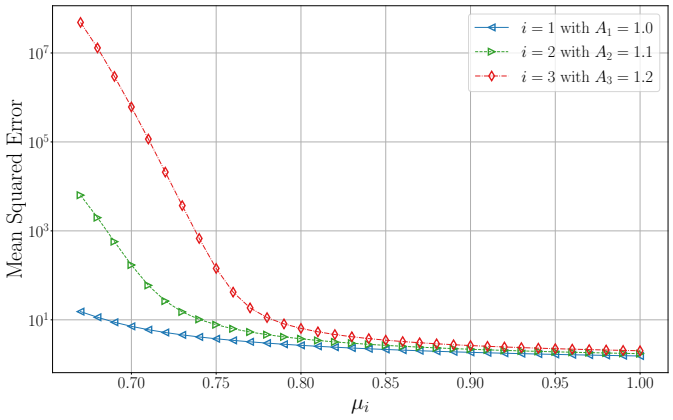


Fig. 2. MSE for varying $\mu_i$ while the arrival rate is fixed, i.e., $\lambda_i = 0.65, \forall i$. Different colors represent different type of control systems with system matrices $A_{1,2,3} \in \{1.0, 1.1, 1.2\}$. A higher $A_i$ represents a less stable system that is more challenging to control.

that throttling the sampling rate is counterproductive w.r.t. estimation performance after a certain point, as it causes the controller to receive outdated information. The same applies to high $\lambda_i$ values that are close to the service rate, i.e., as $\rho_i$ approaches 1. This is caused by the increased queuing delays due to FCFS queuing policy that we assume in our scenario.

Additionally, Fig. 2 shows the effect of increasing the service rate for a constant arrival rate $\lambda_i = 0.65, \forall i$. Note that we only plot against $\{\mu_i : 1 \geq \mu_i > \lambda_i\}$. From the figure, it is evident that a higher service rate affects the estimation performance positively, thus leads to a decrease in MSE as $\mu_i$ increases.

### C. Optimization Problem

As introduced in Sec. II, we assume that within a time slot, distribution of multiple resources to each user $i$ translates into an aggregated transmission success probability that is equal to the service rate of the FCFS Geo/Geo/1 queue. Due to the resource constraint, we assume a total service rate of $R$, that is to be distributed among flows[3]. We define a minimization problem where the arrival rates, i.e., $\boldsymbol{\lambda} = [\lambda_1 \ \lambda_2 \ \dots \ \lambda_N]^T$ are given and the distribution of resources, i.e., $\boldsymbol{\mu} = [\mu_1 \ \mu_2 \ \dots \ \mu_N]^T$ is the only optimization variable. As a result, the optimization problem can be formulated as:

$$\begin{aligned} \min_{\boldsymbol{\mu}} \quad & \sum_{i=1}^{N} C_i(\lambda_i, \mu_i) \\ \text{s.t.} \quad & \lambda_i - \mu_i < 0 \quad , \forall i \\ & \sum_{i=1}^{N} \mu_i \leq R. \\ & 0 \leq \mu_i \leq 1, \forall i \end{aligned} \tag{14}$$

with $C_i$ defined as in Eq. (13).

[3]In order to make the optimization problem tractable, we assume that set of feasible arrival and service rates are convex and domain of the problem is $[0, 1]$.

For instance, for $N = 3$ sub-systems with $\boldsymbol{A}_{1,2,3} = \{1.0, 1.1, 1.2\}$, $\boldsymbol{\Sigma}_1 = \boldsymbol{\Sigma}_2 = \boldsymbol{\Sigma}_3 = 1.0$, $\lambda_1 = \lambda_2 = \lambda_3 = 0.5$ and $R = 2.0$, the optimal service rates, i.e., $\boldsymbol{\mu}^*$ are calculated as:

| $i$ | $\lambda_i$ | $\mu_i^*$ |
|---|---|---|
| 1 | 0.5 | $\approx 0.594$ |
| 2 | 0.5 | $\approx 0.673$ |
| 3 | 0.5 | $\approx 0.733$ |

We used GEKKO optimization suite to obtain the optimal values which is an optimization suite based on Python programming language [17]. Note that, as the eigenvalue of a scalar system matrix $\boldsymbol{A_i}$ equals to the matrix itself. From discrete time LTI control systems, we know that the higher the eigenvalue gets beyond 1, it represents a less stable system and thus becomes more challenging to stabilize. Therefore, if we look at the optimal allocation vector $\boldsymbol{\mu}^*$, we observe that the system with the largest eigenvalue is provided with the highest share from the total available service rate, which coincides with our intuition.

## IV. Results and Evaluation

In order to validate the derivations and confirm that we are able to minimize the MSE in the network, we implemented $N = 3$ scalar control sub-systems in a simulation framework. A simulation run is $T = 20000$ time slots long where each run is repeated 2000 times. The system matrices are chosen as $\boldsymbol{A}_{\{1,2,3\}} = \{1.0, 1.1, 1.2\}$ respectively to represent feedback control loops with heterogeneous time-criticalities. The system noise and the input matrix are assumed to be equal for all sub-systems, i.e., $\boldsymbol{\Sigma}_i = 1.0$ and $\boldsymbol{B}_i = 1.0, \forall i$. We assume $\boldsymbol{Q}_i = 1$ and $\boldsymbol{R}_i = 0, \forall i$. That is, we take only the state cost into account but neglect the penalty for control effort. Therefore, from Eq. (5), the optimal feedback gain matrix is determined as $\boldsymbol{L}_i^* = \boldsymbol{A}_i$, which corresponds to deadbeat control strategy.

Next, we select equal packet injection probabilities for all subsystems, i.e., $\lambda_1 = \lambda_2 = \lambda_3 = 0.5$. Moreover, the total available service rate is selected as $R = 2 < N$ to represent a scenario where guaranteeing successful transmission for all users is not possible, i.e., $\exists i : \mu_i < 1$. In such a setting, using the GEKKO optimization suite, we obtained the optimal values for individual service rates $\mu_1^* \approx 0.594, \mu_2^* \approx 0.673, \mu_3^* \approx 0.733$.

Fig. 3 illustrates both the normalized occurrence frequency of AoI during our simulations and the stationary distribution of AoI obtained from Eq. (12) for the selected $\lambda_i$ and $\boldsymbol{\mu}^*$. We observe that the least critical sub-system, namely $i = 1$ with $\boldsymbol{A}_1 = 1.0$, reached age values beyond 70 during 2000 repetitions. On the other hand, due to its higher allocated service rate, $\mu_3$, sub-system 3 did not exceed 30 at all.

In order to validate Eq. (11) and thus the control model, we measured the mean squared estimation error at each AoI value. In Fig. 4, we observe that the averages throughout the simulations match theory for lower AoI values as they are visited much more often than higher AoI values. For example, for sub-system 1, the MSE of simulations at AoI values start

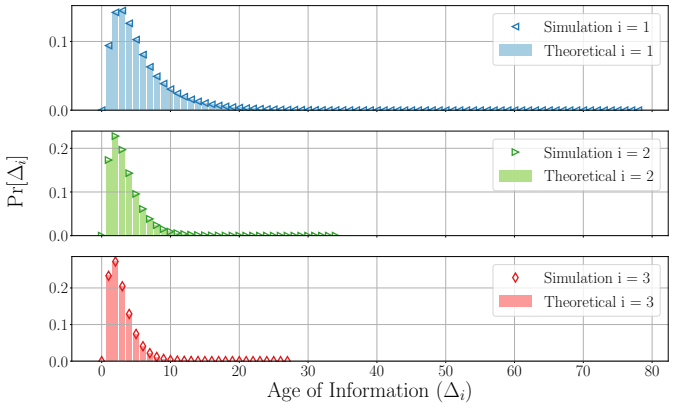


Fig. 3. In a scenario with $N = 3$ control sub-systems, occurrence probability of AoI, $\Pr[\Delta_i]$, and normalized occurrence frequency of $\Delta_i$ during simulations are shown. Equal sampling probability of $\lambda_i = 0.5, \forall i$ is selected. Transmission success probabilities are given as $\boldsymbol{\mu} = [0.605\ 0.672\ 0.723]^T$.

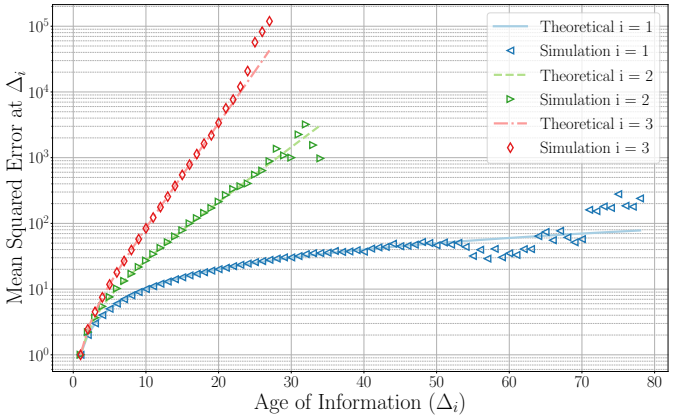


Fig. 4. In a scenario with $N = 3$ control sub-systems, expected and measured MSE of the $i$-th sub-system at age $\Delta_i$ is illustrated. The results show different increase of MSE in AoI for heterogeneous control sub-systems and validate our ability to estimate the MSE successfully given any age. The oscillations towards the right end of the graphs are due to low sample sizes.

to oscillate beyond 50 since the sample size of these data is much lower than of age below 30.

As our goal is to minimize the overall MSE in the network, thus to maximize the estimation performance, we are interested in achieved MSE when the optimal allocation was employed. Therefore, we measured long-term average of the squared estimation error as defined in Eq. (13). In addition, to validate the optimality of the solution, we compared it to other permutations with 3 users without violating the constraints. As resolution within the feasible region, we selected 0.05 to limit our search space. That is, all possible permutations of service rates are simulated, where for each sub-system $i$, the linear space between $\lambda_i$ and 1 is divided into equally distant sub-spaces with a step-size of 0.05. Fig. 5 presents the optimal solution's estimation performance, which is illustrated on the very first column in bold symbols together with the other best performing selected permutations of $(\mu_1, \mu_2, \mu_3)$. We are able to see that none of the allocations is able to beat the obtained

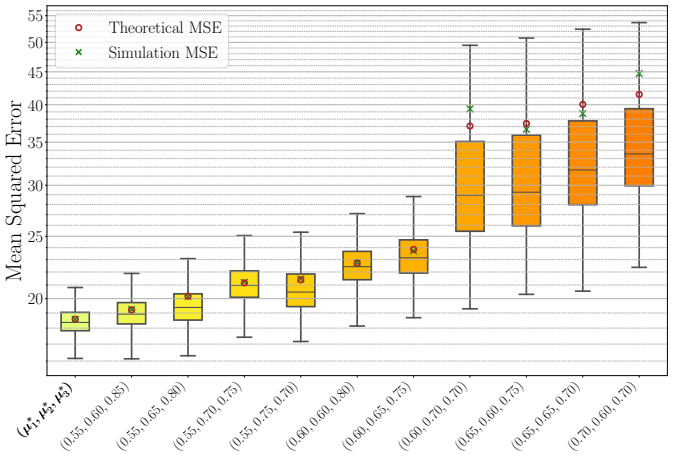


Fig. 5. The resulting mean squared error illustrated when different allocation vectors $\boldsymbol{\mu} = [\mu_1\ \mu_2\ \mu_3]^T$ along the x-axis are applied. Equal sampling probability of $\lambda_i = 0.5, \forall i$ is selected. Outliers are not displayed to avoid visual clutter. Simulation MSE is calculated by taking the average of all 2000 repetitions. The lower and upper whiskers represent the first and third quartiles, respectively.

solution which validates our derivations and claim to maximize the estimation performance.

By looking at the MSE, we are only able to deduce that the estimation accuracy is maximized by applying the optimal resource allocation in the network. However, we are not solely interested in the estimation performance, but also in control performance that is indirectly effected by the estimation process. In fact, suppose a human observing the control systems' states. He or she would be able to judge how the control processes are performing only by looking at the state evolution over time but not at the MSE that is a metric quantifying estimation accuracy. Therefore, in addition to MSE it is important to evaluate the control performance as well. To that end, we measured the average LQG cost in the network during our simulations, $J$, as the QoC metric:

$$J = \sum_{i=1}^{N} F_i, \tag{15}$$

where $F_i$ is defined as in Eq. (7).

Fig. 6 presents the resulting LQG cost in the network when different allocation policies are applied by the centralized scheduler. Similar to Fig. 5, the optimal solution is illustrated in bold next to other best performing permutations within the feasible region. We can observe that our optimal policy, which aims to maximize the estimation accuracy, is also able to reduce the total control cost of sub-systems. This effect can be explained by better decision making at the controller side when provided with more reliable data. This is an intuitive but valuable observation showing how AoI can be used as an intermediate tool to derive age-dependent metrics whose reduction propagates to other performance indicators that are indirectly connected to age.

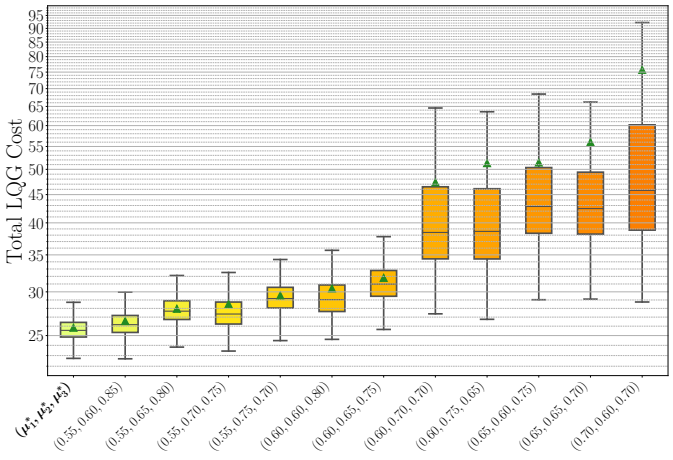


Fig. 6. The resulting linear-quadratic-Gaussian (LQG) cost in the network illustrated when different allocation vectors $\boldsymbol{\mu} = [\mu_1 \ \mu_2 \ \mu_3]^T$ along the x-axis are applied. Equal sampling probability of $\lambda_i = 0.5, \forall i$ is selected. Outliers are not displayed to avoid visual clutter. The triangle marker is placed at the overall average LQG cost throughout 2000 repetitions of each scenario. The lower and upper whiskers represent the first and third quartiles, respectively.

## V. Conclusion

AoI is a metric quantifying information freshness at the receiver in remote monitoring and control scenarios. It has been employed as a cross-layer metric between control and communication in the context of networked control systems. In this work, employ stationary distribution of AoI in discrete time queuing systems where users are feedback control loops. To the best of our knowledge, this is the first work studying centralized scheduling problem for networked control systems where packets have to go through a FCFS queue.

We consider a scenario where multiple, heterogeneous control sub-systems that are sharing a wireless communication channel with packet losses, modeled as an erasure channel. Given discrete time queuing systems with FCFS Geo/Geo/1 discipline, we derive the mean squared error of a remote estimation process given an arrival and a service rate. Thus, we find the optimal distribution of the limited resources of the shared wireless channel. Our results suggest that we are able to maximize the estimation accuracy at the receiver which leads to an increase in control performance. In future work, we are planning to validate our findings with a practical implementation of the considered scenario to validate our theoretical findings in a real-world testbed with software-defined radios.

## Acknowledgment

This work has been carried out with the support of DFG priority programme Cyber-Physical Networking (CPN) with the grant number KE 1863/5-2. In addition, it has been supported in part by ONR N000141812046 and NSF CCF1813078. Moreover, we would like to thank Arled Papa for his valuable input and comments. Last but not least, we would like to thank the reviewers for their helpful comments to improve the quality of the paper.

## References

[1] E. A. Lee, "Cyber physical systems: Design challenges," in *11th IEEE International Symposium on Object and Component-Oriented Real-Time Distributed Computing (ISORC)*, 2008.

[2] S. Kaul, R. Yates, and M. Gruteser, "Real-time status: How often should one update?" in *2012 Proceedings IEEE INFOCOM*, 2012.

[3] I. Kadota, A. Sinha, E. Uysal-Biyikoglu, R. Singh, and E. Modiano, "Scheduling policies for minimizing age of information in broadcast wireless networks," *IEEE/ACM Transactions on Networking*, 2018.

[4] A. M. Bedewy, Y. Sun, and N. B. Shroff, "Minimizing the age of information through queues," *IEEE Transactions on Information Theory*, 2019.

[5] R. Talak, S. Karaman, and E. Modiano, "Minimizing age-of-information in multi-hop wireless networks," in *55th Annual Allerton Conference on Communication, Control, and Computing (Allerton)*, 2017.

[6] S. Farazi, A. G. Klein, J. A. McNeill, and D. Richard Brown, "On the age of information in multi-source multi-hop wireless status update networks," in *IEEE 19th International Workshop on Signal Processing Advances in Wireless Communications (SPAWC)*, 2018, pp. 1–5.

[7] A. Kosta, N. Pappas, A. Ephremides, and V. Angelakis, "Non-linear age of information in a discrete time queue: Stationary distribution and average performance analysis," in *IEEE International Conference on Communications (ICC)*, 2020.

[8] Y. Inoue, H. Masuyama, T. Takine, and T. Tanaka, "A general formula for the stationary distribution of the age of information and its application to single-server queues," *IEEE Transactions on Information Theory*, 2019.

[9] O. Ayan, H. Murat Gürsu, A. Papa, and W. Kellerer, "Probability analysis of age of information in multi-hop networks," *IEEE Networking Letters*, 2020.

[10] R. D. Yates, "The age of information in networks: Moments, distributions, and sampling," *IEEE Transactions on Information Theory*, 2020.

[11] O. Ayan, M. Vilgelm, M. Klügel, S. Hirche, and W. Kellerer, "Age-of-information vs. value-of-information scheduling for cellular networked control systems," in *Proceedings of the 10th ACM/IEEE International Conference on Cyber-Physical Systems (ICCPS)*, 2019.

[12] O. Ayan, M. Vilgelm, and W. Kellerer, "Optimal scheduling for discounted age penalty minimization in multi-loop networked control," in *IEEE 17th Annual Consumer Communications Networking Conference (CCNC)*, 2020.

[13] M. Klügel, M. H. Mamduhi, S. Hirche, and W. Kellerer, "Aoi-penalty minimization for networked control systems with packet loss," in *IEEE Conference on Computer Communications Workshops (INFOCOM WKSHPS)*, 2019.

[14] M. H. Mamduhi, J. P. Champati, J. Gross, and K. H. Johansson, "Where freshness matters in the control loop: Mixed age-of-information and event-based co-design for multi-loop networked control systems," *Journal of Sensor and Actuator Networks*, 2020.

[15] M. Klugel, M. Mamduhi, O. Ayan, M. Vilgelm, K. H. Johansson, S. Hirche, and W. Kellerer, "Joint cross-layer optimization in real-time networked control systems," *IEEE Transactions on Control of Network Systems*, 2020.

[16] L. Kleinrock, *Queueing systems, part I*. Wiley, New York, 1975.

[17] L. D. R. Beal, D. C. Hill, R. A. Martin, and J. D. Hedengren, "Gekko optimization suite," *Processes*, 2018. [Online]. Available: http://www.mdpi.com/2227-9717/6/8/106

## APPENDIX A
## PROOF OF (3)

Given $\nu_i(t) < t$:

$$\begin{aligned}
\hat{\boldsymbol{x}}_i[t] &= \mathbb{E}\left[\boldsymbol{x}_i[t] \mid \boldsymbol{x}_i[\nu_i(t)]\right] \\
&\overset{(2)}{=} \mathbb{E}\left[\boldsymbol{A}_i\boldsymbol{x}_i[t-1] + \boldsymbol{B}_i\boldsymbol{u}_i[t-1] + \boldsymbol{w}_i[t-1] \mid \boldsymbol{x}_i[\nu_i(t)]\right] \\
&= \mathbb{E}\big[\boldsymbol{A}_i\left(\boldsymbol{A}_i\boldsymbol{x}_i[t-2] + \boldsymbol{B}_i\boldsymbol{u}_i[t-2] + \boldsymbol{w}_i[t-2]\right) \\
&\quad + \boldsymbol{B}_i\boldsymbol{u}_i[t-1] + \boldsymbol{w}_i[t-1] \mid \boldsymbol{x}_i[\nu_i(t)]\big] \\
&= \mathbb{E}\Bigg[\boldsymbol{A}_i^{t-\nu_i(t)}\boldsymbol{x}_i(\nu_i(t)) + \sum_{q=1}^{t-\nu_i(t)} \boldsymbol{A}_i^{q-1}\boldsymbol{B}_i\boldsymbol{u}_i[t-q] \\
&\quad + \sum_{q=1}^{t-\nu_i(t)} \boldsymbol{A}_i^{q-1}\boldsymbol{w}_i[t-q] \mid \boldsymbol{x}_i[\nu_i(t)]\Bigg] \\
&= \boldsymbol{A}_i^{t-\nu_i(t)}\boldsymbol{x}_i[\nu_i(t)] + \sum_{q=1}^{t-\nu_i(t)} \boldsymbol{A}_i^{q-1}\boldsymbol{B}_i\boldsymbol{u}_i[t-q] \quad \square
\end{aligned}$$

## APPENDIX B
## PROOF OF (9)

Given $\nu_i(t) < t$ and $\Delta_i[t] \triangleq t - \nu_i[t]$:

$$\begin{aligned}
&\mathbb{E}\left[\|\boldsymbol{e}_i[t]\|^2 \mid \boldsymbol{x}_i[\nu_i[t]]\right] \\
&\overset{(8)}{=} \mathbb{E}\left[\left(\boldsymbol{x}_i[t] - \hat{\boldsymbol{x}}_i[t]\right)^T\left(\boldsymbol{x}_i[t] - \hat{\boldsymbol{x}}_i[t]\right) \mid \boldsymbol{x}_i[\nu_i[t]]\right] \\
&\overset{(2),(3)}{=} \mathbb{E}\left[\left(\sum_{q=1}^{\Delta_i[t]} \boldsymbol{A}_i^{q-1}\boldsymbol{w}_i[t-q]\right)^T\left(\sum_{q=1}^{\Delta_i[t]} \boldsymbol{A}_i^{q-1}\boldsymbol{w}_i[t-q]\right)\right] \\
&= \mathbb{E}\left[\sum_{q=1}^{\Delta_i[t]} \left(\boldsymbol{w}_i[t-q]\right)^T\left(\boldsymbol{A}_i^{q-1}\right)^T \sum_{q=1}^{\Delta_i[t]} \boldsymbol{A}_i^{q-1}\boldsymbol{w}_i[t-q]\right] \\
&\overset{\text{A}}{=} \mathbb{E}\left[\sum_{q=1}^{\Delta_i[t]} \left(\boldsymbol{w}_i[t-q]\right)^T\left(\boldsymbol{A}_i^{q-1}\right)^T \boldsymbol{A}_i^{q-1}\boldsymbol{w}_i[t-q]\right] \\
&\overset{\text{B}}{=} \mathbb{E}\left[\sum_{q=1}^{\Delta_i[t]} \mathsf{tr}\left((\boldsymbol{A}_i^{q-1})^T\boldsymbol{A}_i^{q-1}\boldsymbol{\Sigma}_i\right)\right] \\
&= \mathbb{E}\left[\sum_{q=0}^{\Delta_i[t]-1} \mathsf{tr}\left((\boldsymbol{A}_i^{q})^T\boldsymbol{A}_i^{q}\boldsymbol{\Sigma}_i\right)\right] \quad \square
\end{aligned}$$

A: Noise vectors are i.i.d. thus uncorrelated.
B: Expectation of a quadratic norm of a random vector $\boldsymbol{v}$ with covariance matrix $\boldsymbol{\Sigma}_{\boldsymbol{v}}$ is $\mathbb{E}[\boldsymbol{v}^T\boldsymbol{M}\boldsymbol{v}] = (\mathbb{E}[\boldsymbol{v}])^T\boldsymbol{M}\mathbb{E}[\boldsymbol{v}] + \mathsf{tr}(\boldsymbol{M}\boldsymbol{\Sigma}_{\boldsymbol{v}})$.